J|A|C|S ARTICLES

Published on Web 11/03/2009

Functional Roles of a Structural Element Involving Na^+-π Interactions in the Catalytic Site of T1 Lipase Revealed by Molecular Dynamics Simulations

Yohsuke Hagiwara,[†,‡] Hiroyoshi Matsumura,[§] and Masaru Tateno*[,†,‡]

Center for Computational Sciences, University of Tsukuba, Tennodai 1-1-1, Tsukuba Science City, Ibaraki 189-0001, Japan, Graduate School of Pure and Applied Sciences, University of Tsukuba, Tennodai 1-1-1, Tsukuba, Ibaraki 305-8571, Japan, and Department of Applied Chemistry, Graduate School of Engineering, Osaka Univeristy, Yamada-oka 2-1, Suita, Osaka 565-0871, Japan

Received May 6, 2009; E-mail: tateno@ccs.tsukuba.ac.jp

Abstract: Interactions between metal ions and π systems (metal-π interactions) are known to confer significant stabilization energy. However, in biological systems, few structures with metal-π coordination have been determined; thus, its roles must still be elucidated. The cation-π interactions are not correctly described by current molecular mechanics even when using a polarizable force field, and thus they require quantum mechanical calculations for accurate estimation. However, the huge computational costs of the latter methodologies prohibit long-time molecular dynamics (MD) simulations. Accordingly, we developed a novel scheme to obtain an effective potential for calculating the interaction energy with an accuracy comparable to that of advanced ab initio calculations at the CCSD(T) levels, and with computational costs comparable to those of conventional MM calculations. Then, to elucidate the functional roles of the Na^+-phenylalanine (Phe) complex in the catalytic site of T1 lipase, we performed MD simulations in the presence/absence of the accurate Na^+-π interaction energy. A comparison of these MD simulations revealed that a significantly large enthalpy gain in Na^+-Phe16 substantially stabilizes the catalytic site, whereas a water molecule could not be substituted for Na^+ for sufficient stabilization energy. Thus, the cation-π interaction in the lipase establishes a remarkably stable core structure by combining a hydrophobic aromatic ring and hydrophilic residues, of which the latter form the catalytic triad, thereby contributing to large structural changes from the complex with ligands to the free form of the lipase. This is the first report to elucidate the detailed functional mechanisms of Na^+-π interactions.

1. Introduction

The interaction between a cation and an aromatic ring, referred to as the cation-π interaction, is one of the strongest noncovalent forces, and is widely observed in biological macromolecules.[1] Tryptophan (Trp), phenylalanine (Phe), and tyrosine (Tyr) can provide π electrons for the interactions, while arginine (Arg) and lysine (Lys) participate in the interactions as cations. Statistical analyses of data in the Protein Data Bank have shown that such interactions exist at a high frequency of 1 per 77 amino acid residues, and that 26% of Trp residues are involved in cation-π interactions with Arg or Lys.[2] Such Trp/Phe/Tyr−Arg/Lys interactions contribute to the regulation of various structural and functional properties of biological macromolecules, e.g., structural stability, enzymatic reactions, and ligand-protein recognition.[1−6] Furthermore, metal cations such as Na^+ and K^+, which are typically abundant inside/outside cells in living organisms, can also participate in cation-π interactions. In fact, the formation of metal cation complexes with those amino acids has been shown to yield substantial stabilization energy in the gas phase.[7−13] In aqueous solutions, it has been confirmed that the metal cations preferably bind to the amino acids, overcoming the significant desolvation energy of the metals.[2,14−16] However, despite their importance, only a few experimental structures involving metal-π interactions, such as

[†] Center for Computational Sciences, University of Tsukuba.
[‡] Graduate School of Pure and Applied Sciences, University of Tsukuba.
[§] Department of Applied Chemistry, Graduate School of Engineering, Osaka Univeristy.

(1) Ma, J. C.; Dougherty, D. A. *Chem. Rev.* **1997**, *97*, 1303–1324.
(2) Dougherty, D. A. *Science* **1996**, *271*, 163–168.
(3) Meyer, E. A.; Castellano, R. K.; Diederich, F. *Angew. Chem., Int. Ed. Engl.* **2003**, *42*, 1210–1250.
(4) Chan, D. I.; Prenner, E. J.; Vogel, H. J. *Biochim. Biophys. Acta* **2006**, *1758*, 1184–1202.
(5) Dougherty, D. A. *J. Nutr.* **2007**, *137*, 1504S–1508S, discussion 1516S-1517S.
(6) Gallivan, J. P.; Dougherty, D. A. *Proc. Natl. Acad. Sci. U. S. A.* **1999**, *96*, 9459–9464.
(7) Siu, F. M.; Ma, N. L.; Tsang, C. W. *J. Am. Chem. Soc.* **2001**, *123*, 3397–3398.
(8) Dunbar, R. C. *J. Phys. Chem. A* **2000**, *104*, 8067–8074.
(9) Ruan, C. H.; Rodgers, M. T. *J. Am. Chem. Soc.* **2004**, *126*, 14600–14610.
(10) Ryzhov, V.; Dunbar, R. C.; Cerda, B.; Wesdemiotis, C. *J. Am. Soc. Mass Spectrom.* **2000**, *11*, 1037–1046.
(11) Gapeev, A.; Dunbar, R. C. *Int. J. Mass Spectrom.* **2003**, *228*, 825–839.
(12) Gapeev, A.; Dunbar, R. C. *J. Am. Chem. Soc.* **2001**, *123*, 8360–8365.
(13) Kish, M. M.; Ohanessian, G.; Wesdemiotis, C. *Int. J. Mass Spectrom.* **2003**, *227*, 509–524.
(14) Meadows, E. S.; De Wall, S. L.; Barbour, L. J.; Gokel, G. W. *J. Am. Chem. Soc.* **2001**, *123*, 3092–3107.

 © 2009 American Chemical Society

Na^+-Trp and Cs^+-Trp/Phe, have been determined to date.[17−21] Cs^+-Trp/Phe interactions are observed in the active sites of enzymes, implying their participation in catalysis.[19−21] In contrast, with respect to Na^+, the identified binding sites are distant from the active sites in the previously determined protein structures,[17,18] and thus the functional roles of the Na^+-π interactions are still obscure.

Thermoalkalophilic lipases are present in several thermophilic aerobic bacteria, and they exhibit optimal activity for the hydrolysis of triglycerides at 60−75 °C and pH 8−10.[22] Recently, we have determined the crystal structure of a thermoalkalophilic lipase from *Geobacillus zalihae* strain T1 (T1 lipase).[23] It should be noted here that the active site of this lipase has the Na^+-Phe coordination. However, the functional roles of this metal-π interaction, as well as those of the Na^+-Trp and Cs^+-Trp/Phe interactions, remain to be elucidated. In order to understand the roles of this interaction, we performed molecular dynamics (MD) simulations of T1 lipase in the absence/presence of the accurate Na^+-π interaction energy. As a result, standard molecular mechanics (MM) representations for the Na^+-Phe coordination could not reproduce the structure of the catalytic site in the MD simulation. Furthermore, even when polarizable force field representations were used, artifactitious structural transitions, which are not observed in the crystal structures, were induced in the MD simulation.

Therefore, the accurate description of cation-π interactions is a challenging task in MM calculations, which are required to perform long-time MD simulations. In the present study, we developed a novel scheme to provide an accurate description of the stabilization energy of cation-π interactions. We propose the functional roles of the Na^+-Phe interactions in T1 lipase, by comparing the following two types of MD simulations: one where the novel scheme is used and the other where the standard force field representations are used in the absence/presence of a polarizable force field. Our results revealed that the Na^+-Phe16 interactions are significantly responsible for stabilization of the catalytic site, by exploiting the large energy gain. In the previous crystallographic analysis, instead of the Na^+-Phe complex, different possibilities, such as the H_2O-Phe complex, could not be absolutely dismissed. In the present work, we suggest that Na^+ cannot be energetically substituted for a water molecule in the catalytic site of T1 lipase.

With respect to the functional roles of the Na^+-π interactions, Phe16 is conserved among the thermoalkalophilic lipases from various species, and is crucial for establishing hydrophobic interactions with the ligand for catalysis.[24] Alternatively, in the absence of the ligand, Phe16 is located near hydrophilic amino acids such as serine (Ser) 113 and histidine (His) 358, which are both essential to the catalysis, in an environment with the buried protein structure of T1 lipase. Interactions between hydrophobic and hydrophilic amino acid residues are, in principle, unfavorable in terms of the free energy. However, cation-π interactions such as those in the Na^+-Phe16 complex in T1 lipase facilitate the establishment of a stable core structure by the combination of a hydrophobic aromatic ring and hydrophilic amino acid residues in the buried protein structure. This may further contribute to the dramatic conformational changes from the complex of the lipase and the reaction products to the free form of the lipase.

2. Materials and Methods

2.1. Description of the Total Energy Function. We introduce a function corresponding to the "electron density", $\rho(\mathbf{r})$, derived from an atom using a Gaussian-type function.

$$\rho(\mathbf{r}) = \sum_{i}^{N_{\text{atoms}}} q_i\, a_{i,x} \exp(-a_{i,x}^2(x - x_i)^2)\, a_{i,y} \exp(-a_{i,y}^2(y - y_i)^2)\, a_{i,z} \exp(-a_{i,z}^2(z - z_i)^2) \quad (1)$$

Here, $\mathbf{r}$ and q_i are the position vector of the nucleus of an atom i and the number of electrons of atom i, respectively, and $a_{i,\lambda}$ ($\lambda = x, y, z$) are parameters that regulate the distributions of electrons specific to the x, y, and z directions. The anisotropic qualities of the electron density can be considered when different values are assigned to each $a_{i,\lambda}$. Here, $\rho(\mathbf{r})$ is referred to as the density distribution function. The function is not necessarily a Gaussian-type function; other functions, such as the Slater-type function, can be used to describe the density distribution function.

Next, an effective functional is used to describe the electrostatic interaction energy to evaluate metal-π interactions. One can, in general, utilize any desired potential functional depending on the interaction; in this report, we employ the following functional to describe Na^+-π interactions (the reason why we used this functional is discussed in the Results and Discussion):

$$E_{\text{elec}} = \int \left(\frac{q_i \rho(\mathbf{r})}{r} \times f_{\text{cut}} \right) d\mathbf{r} \quad (2)$$

Here, q_i represents the partial charge of Na^+ (i.e., +1) and r represents the distance between Na^+ and the position represented by $\mathbf{r}$. A cutoff function f_{cut} is used to avert the divergence of physical quantities that occurs for significantly small values of r. α is a parameter chosen to determine the cutoff range.

$$f_{\text{cut}} = \exp\left(-\frac{\alpha}{r}\right) \quad (3)$$

To perform the integration in eq 2 numerically, the formulation is written using a grid-based description

$$E_{\text{elec}} = \sum_{\mathbf{r} \in \text{Phe}} w(\mathbf{r}) \left(\frac{q_i \rho(\mathbf{r})}{r} \times f_{\text{cut}} \right) \quad (4)$$

The grid points $\mathbf{r}$ are distributed around the atoms involved in the aromatic ring, and $w(\mathbf{r})$ represents the weight of each grid corresponding to a small volume $d\mathbf{r}$ in the integral. It has been shown that the major components of the Na^+-π interaction energy are electrostatic and induction energies, and that the contribution of the van der Waals interaction is negligible.[25] Accordingly, as a total energy function, we can employ the potential energy function

(15) Hu, J.; Barbour, L. J.; Gokel, G. W. *Proc. Natl. Acad. Sci. U. S. A.* **2002**, *99*, 5121–5126.
(16) Costanzo, F.; Della Valle, R. G. *J. Phys. Chem. B* **2008**, *112*, 12783–12789.
(17) Wouters, J. *Protein Sci.* **1998**, *7*, 2472–2475.
(18) Wouters, J.; Maes, D. *Acta Crystallogr.* **2000**, *56*, 1201–1203.
(19) Kooystra, P. J.; Kalk, K. H.; Hol, W. G. *Eur. J. Biochem.* **1988**, *177*, 345–349.
(20) Liaw, S. H.; Kuo, I.; Eisenberg, D. *Protein Sci.* **1995**, *4*, 2358–2365.
(21) Labesse, G.; Ferrari, D.; Chen, Z. W.; Rossi, G. L.; Kuusk, V.; McIntire, W. S.; Mathews, F. S. *J. Biol. Chem.* **1998**, *273*, 25703–25712.
(22) Demirjian, D. C.; Moris-Varas, F.; Cassidy, C. S. *Curr. Opin. Chem. Biol.* **2001**, *5*, 144–151.
(23) Matsumura, H.; Yamamoto, T.; Leow, T. C.; Mori, T.; Salleh, A. B.; Basri, M.; Inoue, T.; Kai, Y.; Rahman, R. N. *Proteins* **2008**, *70*, 592–598.
(24) Carrasco-Lopez, C.; Godoy; de Las Rivas, B.; Fernandez-Lorente, G.; Palomo, J. M.; Guisan, J. M.; Fernandez-Lafuente, R.; Martinez-Ripoll, M.; Hermoso, J. A. *J. Biol. Chem.* **2009**, *284*, 4365–4372.

defined in Amber 9.0[26] with the modification that the electrostatic term is replaced with eq 2. Thus, the energy function that describes the total energy of the system involving the metal-π interaction is written as follows:

$$E = E_{\text{bonded}} + E_{\text{elec}} + \sum_{i<j}^{\text{atoms}} \left(\frac{A_{ij}}{R_{ij}^{12}} - \frac{B_{ij}}{R_{ij}^{6}} \right) \quad (5)$$

2.2. Optimization of Parameters of the Density Distribution Function. Since eq 2 depends on the density distribution function $\rho(\mathbf{r})$, which is supposed to be the total electron density, the parameter values in the function should be determined through a fitting procedure such that the total energy curves obtained by highest level ab initio calculations before this fitting are reproduced by eq 5. This optimization of parameters in the function was performed as follows. First, the potential energy curves were obtained for model structures using calculations at the coupled-cluster with singles, doubles, and perturbative triples (CCSD(T)) levels, for which the accuracy is known to be dependent on the basis set; thus, a larger basis set is required to estimate the energy values accurately. However, the computational cost increases markedly as the basis set becomes larger. In this study, the CCSD(T) energy is estimated at a basis set limit that mimics the energy calculated using a complete basis set, by a procedure proposed by Tsuzuki, et al.[27] We also performed conventional density functional theory (DFT) calculations at the B3LYP/6-311+G(d,p) level for the Na^+-benzene system, and found that the DFT slightly overestimates the interaction energy.[28] Accordingly, we employed the result of the CCSD(T) calculations as the reference in this study.

Second, we fitted the values obtained from the total energy function defined by eq 5 to reproduce the potential energy curve obtained by CCSD(T) calculations at a basis set limit. We employed a simulated annealing (SA) protocol for the fitting, where $a_{i,\lambda}$, which regulates the density distribution function, is used as a variable. At each step of the SA protocol, a set of parameters is obtained; then, the total energy values obtained by eq 5 are calculated for the model structures. Subsequently, deviations between the current outputs using eq 5 and the energy values obtained at the CCSD(T) level are evaluated using the Metropolis criteria in the SA protocol. To summarize, our scheme for obtaining an effective potential consists of the following four steps: (i) calculation of $\rho(\mathbf{r})$ for each grid using a parameter set; (ii) calculation of the electrostatic energy using an effective potential that includes $\rho(\mathbf{r})$; (iii) calculation of the total energy using eq 5; and (iv) evaluation of the total energy values obtained in step (iii) and of those obtained from higher-level ab initio calculations performed beforehand.

2.3. Quantum Mechanical Calculations. All ab initio molecular orbital calculations of the Na^+-benzene system were performed using Gaussian 03.[29] Geometry optimization for isolated benzene was performed at the B3LYP/6-311+G(d,p) level, and the optimized structure was used to construct Na^+-benzene complex structures (the atomic coordinates of the optimized structure are shown in the Supporting Information; Table S1). For single point calculations of those structures, we employed a procedure to estimate the CCSD(T) energy at a basis set limit proposed by Tsuzuki et al.[27] For a comparison, single point calculations at the B3LYP/6-311+G(d,p) level were also performed. The basis set superposition error was corrected by the counterpoise method.[30]

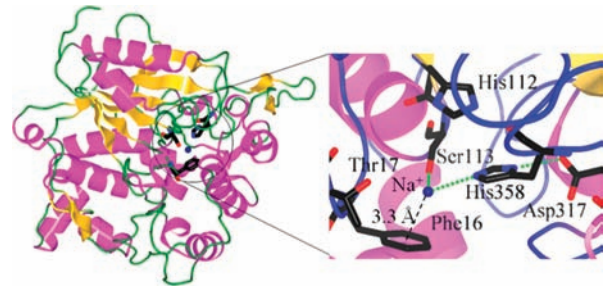

Figure 1. Crystal structure of the *Geobacillus zalihae* T1 lipase (PDB code: 2DSN). Na^+ is depicted as a dark blue sphere. A close-up view of the configuration of the catalytic site is also shown (right panel). In the active site, Na^+ is coordinated to the side chains of Phe16, Ser113, and His358.

2.4. Molecular Dynamics Calculations. All molecular dynamics (MD) simulations were performed using AMBER 9.[26] The ff99 and ff02 force fields were applied to all atoms in the system. Electrostatic interactions were calculated by the particle mesh Ewald method with a dielectric constant of 1.0,[31] and a cutoff of 12 Å was used to calculate the direct space sum for the particle mesh Ewald method. The SHAKE algorithm[32] was used to constrain bond length involving hydrogen atoms. The time step for the integration was set to 1 fs. The temperature and pressure were controlled at 300 K and 1.013×10^5 Pa, respectively, using the Berendsen algorithm.[33]

Initial coordinates of the protein were taken from the crystal structure of T1 lipase (the Protein Data Bank accession code 2DSN[23] Figure 1). First, hydrogen atoms were added to the crystal structure using the LEAP module implemented in AMBER 9. The positions of the added hydrogen atoms were optimized by the steepest descent method; then, the optimization was performed for all protein atoms. The protein was subsequently immersed in a box of water molecules consisting of 54,357 atoms modeled by TIP3P. Two Na^+ ions were added to neutralize the system. Thus, the total atom number of the solvated protein system was 60 334. To relax the configuration of the solvent water molecules, the MD simulation was performed for 10 ps at 300 K, where a harmonic constraint was applied to all protein and Na^+ atoms with a force constant of 500 kcal mol^{-1} $Å^{-2}$. With respect to the density distribution function, the optimized values of a_x, a_y, and a_z for carbon atoms were 0.758, 0.758, and 0.864 Å, respectively, and those for hydrogen atoms were 0.166, 0.166, and 0.933 Å, respectively. α in the cutoff function (eq 3) was taken as 1.0×10^{-5}. A cube, for which the center is located on the center of mass of the aromatic ring, was generated; the volume of the cube was 10^3 $Å^3$, where the grid-point space inside the cube was set to 0.2 Å. Accordingly, the number of grid points involved in the cube was 125 000.

3. Results and Discussion

3.1. Evaluation of Force Fields. *Geobacillus zalihae* lipase (T1 lipase) is a thermoalkalophilic lipase that hydrolyzes triglycerides into fatty acids and glycerol. The crystal structure of T1 lipase revealed that the Na^+ at the active site binds the side chain of Phe16 via a cation-π interaction (Figure 1).

It is well-known that the induction energy, which can be described in polarizable force fields, is a major origin of the cation-π interaction.[1,2,25,34−39] In our previous study, we evaluated a polarizable force field, AMBER ff02,[26] for describing

(25) Soteras, I.; Orozco, M.; Luque, F. J. *Phys. Chem. Chem. Phys.* **2008**, *10*, 2616–2624.
(26) Case, D. A.; Cheatham, T. E.; Darden, T.; Gohlke, H.; Luo, R.; Merz, K. M.; Onufriev, A.; Simmerling, C.; Wang, B.; Woods, R. J. *J. Comput. Chem.* **2005**, *26*, 1668–1688.
(27) Tsuzuki, S.; Uchimaru, T.; Mikami, M. *J. Phys. Chem. A* **2006**, *110*, 2027–2033.
(28) Tateno, M.; Hagiwara, Y. *J. Phys.: Condens. Matter* **2009**, *21*, 064243.
(29) Frisch, M. J. et al. 2003 *Gaussian 03* Gaussian, Inc., Pittsburgh, PA.
(30) Boys, S. F.; Bernardi, F. *Mol. Phys.* **1970**, *19*, 553–566.
(31) York, D. M.; Darden, T. A.; Pedersen, L. G. *J. Chem. Phys.* **1993**, *99*, 8345–8348.
(32) Ryckaert, J. P.; Ciccotti, G.; Berendsen, H. J. C. *J. Comput. Phys.* **1977**, *23*, 327–341.
(33) Berendsen, H. J. C.; Postma, J. P. M.; Vangunsteren, W. F.; Dinola, A.; Haak, J. R. *J. Chem. Phys.* **1984**, *81*, 3684–3690.

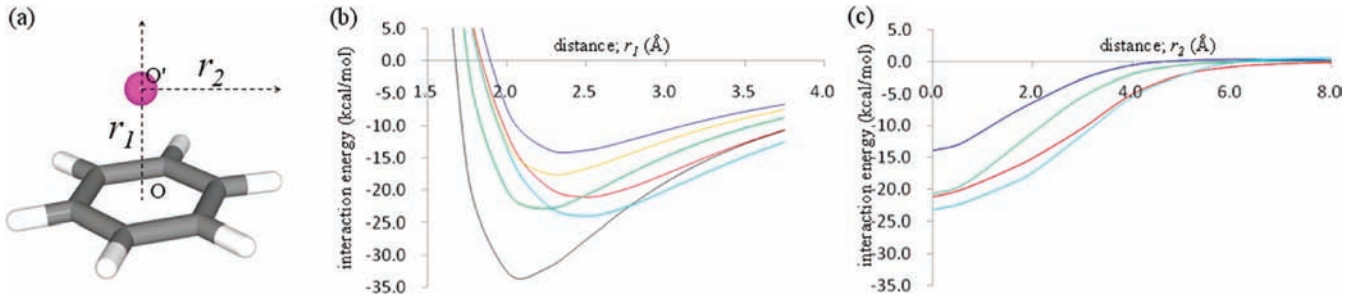

Figure 2. (a) Model structures for Na^+-π interactions, where the metal is placed on a line perpendicular to the benzene ring and passing through the center of mass of the benzene ring *O*. r_1 denotes the distance of Na^+ from *O*. *O′* is the point wherer_1 is 2.5 Å (which is the optimal distance of r_1 in the potential curve), and r_2 denotes the distance of Na^+ from *O′* along a line parallel to the benzene ring and passing through *O′*. Energy profiles of interaction energies of Na^+ and the benzene ring with respect to (b) r_1 and (c) r_2. The interaction energies of a Na^+-benzene system obtained by CCSD(T) at the basis set limit, DFT, and MM using a nonpolarizable force field are shown in red, light blue, and blue. The green line was obtained by MM calculations using a polarizable force field. In (b), the two energy curves shown in black and orange were obtained by MM calculations using optimized parameter sets; the energy curve to be fitted in larger distance regions ($r_1 > 2.5$ Å) is shown in black, and that fitted in shorter distance regions ($r_1 < 2.0$ Å) is shown in orange.

the Na^+-π interactions.[28] In the previous evaluation, we used the geometries of the Na^+-π complex, where the Na^+ was placed along the axis perpendicular to the aromatic ring, and calculated the potential energy curve with respect to r_1, which is the distance between Na^+ and the center of mass of the aromatic ring *O* shown in Figure 2a. In this study, to consider other configurations, we constructed model structures where Na^+ was placed on the axis that is parallel to the aromatic ring (Figure 2a). In the figure, *O′* denotes the cross point of the two axes (r_1 is 2.5 Å), and r_2 is defined as the distance between Na^+ and *O′*. Figure 2, parts b and c, shows the serious discrepancies between the force field calculations and the CCSD(T) calculations. Several studies have also reported the difficulties in the accurate estimation of the cation-π interactions by polarizable force fields.[25,40,41]

Accordingly, in MD simulations using the polarizable force field, such significant discrepancies in the potential energy may cause artifactitious deviations of the structures around the Na^+-Phe interactions from the experimental conformation. In fact, in the resultant two-dimensional free energy profile with respect to the distance between Na^+ and the center of mass of the aromatic ring of Phe16, and that between Na^+ and N_ϵ of His358, the minimum corresponds to a structure that is not observed in the crystal structure (Figures 3a and 4a). The inconsistency with the experimental result would be caused by the inaccurate potential curve, where the minimum is shifted toward the shorter distance (a detailed discussion is provided in the Supporting Information). Thus, we attempted to optimize the atomic polarizabilities such that the energy potential with respect to the distance r_1 (defined in Figure 2a) fits well to the energy potential obtained using CCSD(T) calculations at the basis set limit. However, none of the parameter values could reproduce the referenced energy potential (see Supporting Information).

We previously evaluated the standard nonpolarizable force field (AMBER ff99),[26] and found better consistency with the CCSD(T) calculations in terms of the shape of the potential curve for the Na^+-benzene systems than the polarizable force field.[28] This is consistent with the previous study; i.e., the optimized geometry of the Na^+-benzene complex calculated by nonpolarizable force fields was quite consistent with the optimized one generated by DFT calculations.[42] However, the minimum energy values differed by ~10 kcal/mol between the two force fields (Figure 2b). Such a significant difference in the minimum energy was also reported in the K^+-benzene complex.[43] Thereby, in MD simulations using the standard nonpolarizable force field, artifactitious structural deviations may occur with respect to the Na^+-Phe complex. In fact, the free energy profile calculated using the 2-ns MD trajectory shows wide fluctuations of the Na^+-coordinated structure and the existence of some (semi) stable structures, which are not observed in the crystal structure (Figure 3b). The formation of the incorrect structures (Figure 4b−d) may be caused by the insufficient stabilization energy estimated by the force field; the Na^+-Phe16 interaction competes with the Na^+-His112 (N^δ) interaction, inducing the dissociation of Na^+ from Phe16. The detailed mechanisms are discussed in the Supporting Information.

3.2. MD Simulation Involving the Grid-Based Representation for the Na^+-π Interaction. In this manner, we have shown that the current MM calculations cannot reproduce cation-π interactions. However, with respect to the interactions of Na^+ with functional groups lacking aromatic properties, it has been reported that the MM calculations provide results consistent with experimental data.[44−46] These facts suggest that the structural deviations observed in the above-mentioned simulations would be avoided by the refinement of the description of only cation-π interactions. Accordingly, we developed a novel scheme to accurately describe such interactions to investigate the functional roles of the Na^+-Phe16 complex in T1 lipase. Our scheme, described in the Materials and Methods, was applied to evaluate the Na^+-π interaction in the catalytic site of T1 lipase.

(34) Cubero, E.; Luque, F. J.; Orozco, M. *Proc. Natl. Acad. Sci. U. S. A.* **1998**, *95*, 5976–5980.
(35) Zacharias, N.; Dougherty, D. A. *Trends. Pharmacol. Sci.* **2002**, *23*, 281–287.
(36) Kim, D.; Hu, S.; Tarakeshwar, P.; Kim, K. S.; Lisy, J. M. *J. Phys. Chem. A* **2003**, *107*, 1228–1238.
(37) Lee, J. Y.; Lee, S. J.; Choi, H. S.; Cho, S. J.; Kim, K. S.; Ha, T. K. *Chem. Phys. Lett.* **1995**, *232*, 67–71.
(38) Kim, K. S.; Lee, J. Y.; Lee, S. J.; Ha, T. K.; Kim, D. H. *J. Am. Chem. Soc.* **1994**, *116*, 7399–7400.
(39) Tsuzuki, S.; Honda, K.; Uchimaru, T.; Mikami, M.; Fujii, A. *J. Phys. Chem. A* **2006**, *110*, 10163–10168.
(40) Chipot, C.; Maigret, B.; Pearlman, D. A.; Kollman, P. A. *J. Am. Chem. Soc.* **1996**, *118*, 2998–3005.
(41) Minoux, H.; Chipot, C. *J. Am. Chem. Soc.* **1999**, *121*, 10366–10372.
(42) Wouters, J. *J. Comput. Chem.* **2000**, *21*, 847–855.
(43) Ponder, J. W.; Case, D. A. *Adv. Protein Chem.* **2003**, *66*, 27–85.
(44) Noskov, S. Y.; Roux, B. *J. Gen. Physiol.* **2007**, *129*, 135–143.
(45) Luzhkov, V. B.; Aqvist, J. *Biochim. Biophys. Acta* **2005**, *1747*, 109–120.
(46) Khalili-Araghi, F.; Gumbart, J.; Wen, P. C.; Sotomayor, M.; Tajkhorshid, E.; Schulten, K. *Curr. Opin. Struct. Biol.* **2009**, *19*, 128–137.

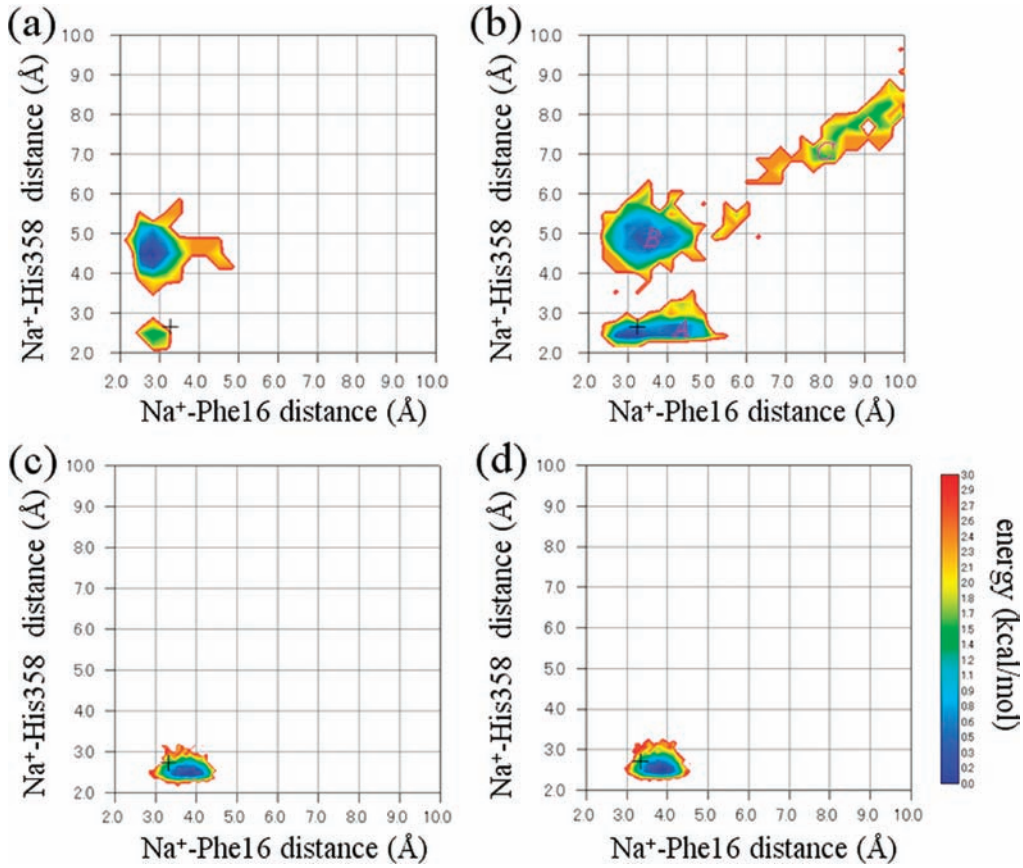

Figure 3. Free energy landscapes obtained by a standard MD simulation of T1 lipase using a polarizable force field (a), a nonpolarizable force field (b), and a force field involving our grid-based representation of the electrostatic interaction calculated for 2-ns (c) and 5-ns (d). The vertical axis shows the distance between Na^+ and N_ϵ of His358, and the horizontal axis the distance between Na^+ and the center of mass of the side chain of Phe16. A cross (+) represents the crystal structure. In (b), *A*, *B*, and *C* represent (semi) stable states in the free energy landscape obtained in the standard MD simulation.

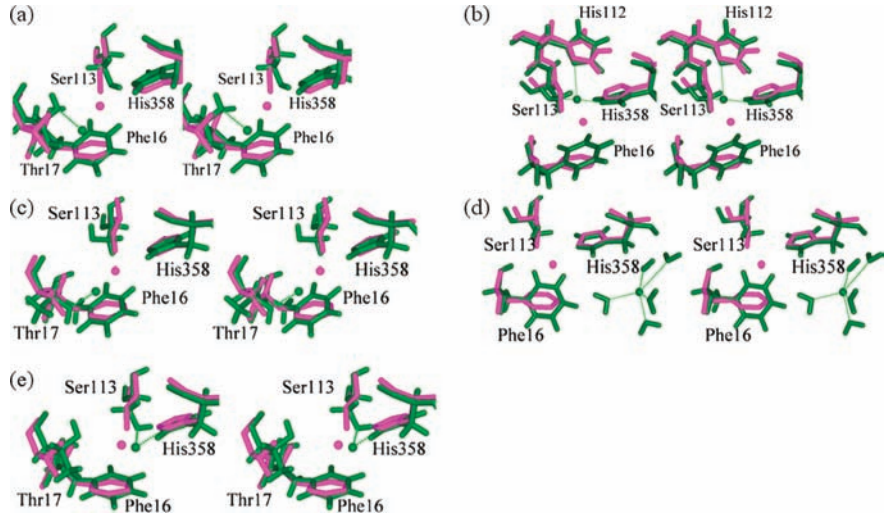

Figure 4. Conformations of the most stable state in Figure 3a (a), those of the *A* (b), *B* (c), and *C* (d) states shown in Figure 3b, and those of the most stable state in Figure 3d (e). The crystal structure of the *Geobacillus zalihae* lipase is colored magenta, and the snapshots of the MD simulations are green.

As described in the Materials and Methods section 2.1, our energy function (eq 5) includes the electrostatic interaction (eq 2) based on the density distribution function (eq 1), and fits the CCSD(T) potential curves well through the optimization of the Na^+-π interaction, as shown in Figure 5. Here, eq 2 represents the Coulomb interaction, and thus, the induction energies are not explicitly considered in our energy function, eq 5. To compensate for it, we combined eq 1, which includes the parameters to correct the errors of the force field, with eq 2. This allowed us to reproduce the accurate energy potential without estimating the accurate induction energies. In this meaning, eq 2 is also used for the correction of the force field potential. One may employ an alternative equation, but the simplicity of eq 2 is attractive for computation.

A few empirical approaches analogous to our scheme have been proposed to date; in those schemes, representations to

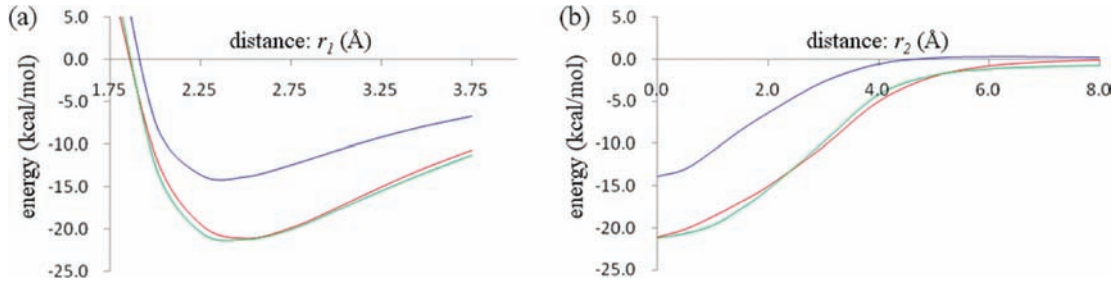

Figure 5. The potential energy curves with respect to (a) r_1 and (b) r_2 (Å). The potential curves obtained by CCSD(T) calculations at the basis set limit (red), MM (blue), and our scheme (green).

mimic the spatial electron distribution are used. One is the "off-atom" charge model, where a few extra charge points are placed on off-atom positions.[47−50] A more straightforward way to mimic the density distribution is to use Gaussian functions, i.e., the Gaussian electrostatic model (GEM).[51,52] In this scheme, the approximate density function for each molecule (monomer) is fitted to the electron density obtained by ab initio calculations, and is exploited for computing the interaction energy of the complex of the molecules. Its advantage is that it enables us to calculate the individual energies of nonclassical interactions by incorporating the corresponding energy terms into quantum mechanical (QM) Hamiltonians. Thus, GEM is a procedure based on simplified QM calculations. In contrast, in our scheme, the total effects of such nonclassical interactions are included through the optimization, since the parameters are determined so as to reproduce the total interaction energy obtained by advanced ab initio calculations. Thus, our scheme is designed for MM calculations involving long time MD simulations, and is conceptually different from GEM. Moreover, the idea of using Gaussian functions to represent electron distributions has also been utilized to address an issue arising from the treatment of the QM-MM boundary, referred to as the "overpolarization" problem.[53−55] However, for this methodology, no solid scheme to determine the parameter that regulates the width of the charge distribution has been proposed to date. In this manner, our scheme is definitely distinguishable from the previous alternative ones.

We conducted an MD simulation using the obtained energy function. The computation time was comparable to that of a standard MD simulation (Table 1); i.e., the time required for our scheme is 0.18 s/step to calculate one point total energy of the benzene−Na^+ system, when using the SGI Altix 3700 system with an Intel Itanium 2 processor (1.6 GHz). It should be noted here that the time required to perform the MD simulation of the fully solvated system using a standard energy function is 3.26 s/step, and thus the additional time for our grid-based electrostatic evaluation, 0.18 s/step, is negligible in such MD simulations. Thus, the computation time needed to accomplish the MD simulation using our scheme, 3.44 (= 3.26 + 0.18) s/step, is comparable with that using a standard energy function. In comparison with higher level ab initio methods, it is clear that the time required for our scheme is dramatically reduced, even though the accuracy is comparable in both methodologies. In fact, a computation time of 3.95×10^7 s/step is required for CCSD(T) calculations using the aug-cc-pVTZ basis set. Even when our calculation scheme is compared with the method proposed by Tsuzuki et al.[27] to mimic the CCSD(T) calculation at the basis set limit obtained by MP2 calculations with a huge basis set, the CPU time required to calculate our energy function is also significantly reduced, by 10^5-fold.

Table 1. Computational Times Required for the MD Simulations of the Solvated Lipase

method	standard energy function	our scheme	method proposed by Tsuzuki et al.[27]	CCSD(T)[b]
time (s)[a]	3.26	3.44	1.46×10^4	3.95×10^7

[a] Computational time required to perform a 1-step MD simulation of the lipase. [b] CCSD(T) with use of the aug-cc-pVTZ basis set.

We calculated the free energy profile using the 2-ns and 5-ns MD trajectories as shown in Figure 3, parts c and d, respectively. The comparison of these free energy profiles revealed that the free energy calculations converged well. As compared with the profile obtained in the standard MD simulations, the fluctuation of the Na^+-coordinated structure is noticeably reduced; consequently, the interaction between Na^+ and the aromatic ring is significantly stabilized. Thus, the configurations around Na^+ are preserved, as observed in the crystal structure (Figure 4e). The slight deviation from the crystal structure may be due to the partial charge of Na^+: On the basis of our ab initio calculations, we have noticed that the exact value of the atomic charge of Na^+ is slightly less than the conventional value (the formal charge), which was also used in our simulations (+1), since the electron transfer would occur from the aromatic ring to the Na^+. This small inconsistency would be avoided by also applying the grid-based representation and our fitting scheme to Na^+. This extension of our methodology is the next step in the near future.

A comparison of the dihedral angles of $\chi 1$ and $\chi 2$ of Phe16 obtained from three MD simulations also reveals that the accurate description of the Na^+-Phe interaction in the catalytic site substantially contributes to achieving stability and consistency with the experimental structure. In fact, the averaged values of $\chi 1$ and $\chi 2$ obtained from the MD simulation involving our grid-based scheme are close to the experimental values, and

(47) Kaminski, G. A.; Stern, H. A.; Berne, B. J.; Friesner, R. A.; Cao, Y. X. X.; Murphy, R. B.; Zhou, R. H.; Halgren, T. A. *J. Comput. Chem.* **2002**, *23*, 1515–1531.
(48) Mannfors, B.; Palmo, K.; Krimm, S. *J. Phys. Chem. A* **2008**, *112*, 12667–12678.
(49) Cao, Z. X.; Lin, Z. X.; Wang, J.; Liu, H. Y. *J. Comput. Chem.* **2009**, *30*, 645–660.
(50) Dixon, R. W.; Kollman, P. A. *J. Comput. Chem.* **1997**, *18*, 1632–1646.
(51) Cisneros, G. A.; Piquemal, J. P.; Darden, T. A. *J. Chem. Phys.* **2005**, *123*, 044109.
(52) Piquemal, J. P.; Cisneros, G. A.; Reinhardt, P.; Gresh, N.; Darden, T. A. *J. Chem. Phys.* **2006**, *124*, 104101.
(53) Eichinger, M.; Tavan, P.; Hutter, J.; Parrinello, M. *J. Chem. Phys.* **1999**, *110*, 10452–10467.
(54) Das, D.; Eurenius, K. P.; Billings, E. M.; Sherwood, P.; Chatfield, D. C.; Hodoscek, M.; Brooks, B. R. *J. Chem. Phys.* **2002**, *117*, 10534–10547.
(55) Amara, P.; Field, M. J. *Theor. Chem. Acc.* **2003**, *109*, 43–52.

Table 2. Comparison of Dihedral Angles of χ1 and χ2 of Phe16 in the MD Simulations Using ff99, ff02, and Our Grid-Based Representation[a]

	crystal structure[b]	ff99	ff02	our scheme
c1	59.6	71.2 (84.0)	71.3 (68.4)	54.2 (70.1)
c2	67.3	82.7 (143.4)	91.1 (90.4)	79.8 (88.9)

[a] The averaged values (degrees) are shown and the values in parentheses are the variances of those dihedral angles. [b] The crystal structure of T1 lipase.[23]

the fluctuations of the dihedral angles are small, as compared with those obtained from the MD simulations using the standard MM representations (Table 2). This is attributed to the accurate description of the Na^+-Phe interaction by our scheme. Thus, the Na^+-His112 coordination, which is observed in the MD simulation using the nonpolarizable force field, does not appear in the MD simulation involving the grid-based electrostatic interaction. This means that a definite free energy barrier could be present between two minima, each corresponding to the most stable geometries of the Na^+-Phe16/His112 coordination, because the depth of the potential curve of the Na^+-π interactions described using the grid-based representation is lowered by ~10 kcal/mol, as compared with that in the nonpolarizable force field.

3.3. Functional Roles of the Na^+-Phe16 Interaction in T1 Lipase. A comparison of the potential curves described by the ff99 and CCSD(T) calculations reveals that ff99 underestimates the stabilization energy by ~7 kcal/mol at the Na^+-Phe distance of 3.3 Å, which is the atomic distance observed in the crystal structure of T1 lipase. The smaller energy gain estimated by ff99 is supposed to cause the dissociation of Na^+ from Phe16 and the formation of a hydrogen bond between Na^+ and His112, which is not observed in the crystal structure (Figure 4b). Here, we calculated the interaction energy of the H_2O-Phe16 complex via CCSD(T) calculations, using a modeled structure where Na^+ is replaced with the O atom of H_2O (a hydrogen atom of H_2O is oriented toward the aromatic ring in the model). The resultant energy of ~3 kcal/mol is significantly lower than that of ~17 kcal/mol in the case of Na^+, indicating that the 3D structure of the catalytic site would not be maintained in the MD simulation involving the H_2O-Phe16 complex, as well as in that using ff99, as mentioned earlier. In the previous crystallographic analysis, we could not completely rule out the possibility that a water molecule, instead of Na^+, may be located in the catalytic site of T1 lipase.[23] However, the above-mentioned calculations suggest that a water molecule may not be able to substitute for Na^+.

We have shown that inaccurate descriptions of the Na^+-Phe interaction by the polarizable and nonpolarizable force fields yield significant deviations of the calculated structures from the experimental data. In contrast, in the MD simulation involving the accurate description of the Na^+-π interaction in the energy function, the 3D structure of the catalytic site of T1 lipase appears to be remarkably stable. Thus, the Na^+-Phe16 interaction substantially ensures the conformation of the catalytic site in T1 lipase (the substitution of Phe16 observed in other lipases is discussed below).

Recently, the crystal structure of *Geobacillus thermocatenulatus* lipase (BLT2), which is also a thermoalkalophilic lipase, was determined in a complex with ligands. The structure showed that the conformation of the α6- and α7-helices, consisting of approximately 70 amino acid residues, largely changes from a "closed" conformation to an "open" conformation upon ligand binding.[24] A comparison of those two conformations reveals

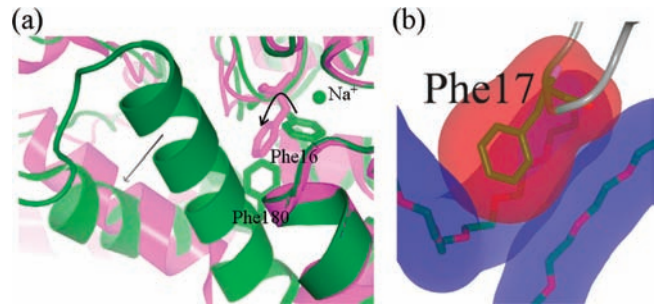

Figure 6. (a) Comparison of the crystal structures of thermoalkalophilic lipases between the open (magenta, PDB code: 2W22) and closed conformations (green, PDB code: 2DSN). Arrows indicate directions of the conformational changes upon ligand binding. In the *Geobacillus zalihae* lipase (closed conformation), Phe16 cannot adopt the conformation observed in the *Geobacillus thermocatenulatus* lipase (open conformation) because of the steric clash between Phe17 in the *Geobacillus thermocatenulatus* lipase (Phe17 corresponds to Phe16 in the *Geobacillus zalihae* lipase) and Phe180 in the *Geobacillus zalihae* lipase. (b) The recognition mode of the ligands by Phe17 in the crystal structure of the *Geobacillus thermocatenulatus* lipase. The ligands surround the side chain of Phe17, forming broad-ranging van der Waals contacts.

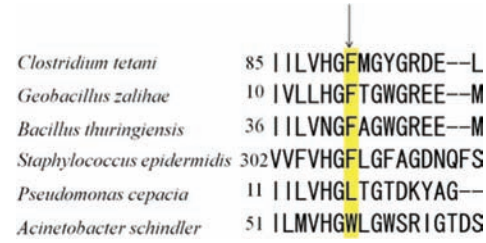

Figure 7. Sequence alignment of the region around Phe16 in the *Geobacillus zalihae* lipase denoted by the arrow among *Clostridium tetani, Bacillus thuringiensis*, *Staphylococcus epidermidis*, *Pseudomonas cepacia*, and *Acinetobacter shindler.*

that Phe16 (in *Geobacillus thermocatenulatus* lipase, the corresponding Phe residue is numbered 17) also undergoes a large conformational change to stabilize the binding of ligands; Phe16 in the open conformation newly establishes broad-ranging van der Waals contacts with its surrounding ligands (Figure 6b). Actually, Phe16 is a conserved amino acid residue involved in the motif Gly-Phe-X-Gly (Figure 7). Note that the conformation of Phe16 observed in the open conformation cannot exist in the closed conformation because of the presence of Phe180 (in *Geobacillus thermocatenulatus*, this Phe residue is numbered as 177) located on the α6-helix (Figure 6a); therefore, the conformations of the Phe16 side chain are completely different between the open and closed states. Thus, the Na^+ probably functions to place the Phe16 side chain at the position observed in the closed state, by the use of the huge amount of enthalpy gain, estimated as approximately -20 kcal/mol.

In a previous study, Phe16 was suggested to function in the formation of a so-called "oxyanion hole" in the open conformation, to stabilize a transition state in the enzymatic reaction; here, the oxyanion hole is composed of the backbone nitrogen atoms of Phe16 and Gln114.[24] Accordingly, the position of the Phe16 side chain changes so that the Phe16 backbone, in turn, is oriented toward the catalytic triad, composed of Ser113, His358, and Asp317 (Figure 6b). Conversely, to form the closed conformation in the absence of the ligand, the Phe16 side chain structurally shifts to form the core structure through interactions with the amino acid residues forming the catalytic triad. However, in principle, direct interactions between a hydrophobic

aromatic ring (Phe16) and hydrophilic amino acid residues (Ser113 and His358) are energetically unfavorable. Therefore, Na^+ may act here to "bridge" the interactions among such amino acid residues, through the formation of the Na^+-π (Phe16), Na^+-O^{γ} (Ser113), and Na^+-N^{δ} (His358) interactions, thereby leading to the establishment of the stable core structure of the active site in the thermoalkalophilic lipase. In fact, a comparison of the present MD simulations indicates that the large enthalpy gain from the Na^+-π interaction is essential to establish the stable 3D structure of the catalytic site in T1 lipase. This leads to further hydrophobic interactions in the environment of the buried protein structure, which may also generate an entropy gain (The formation of a hydrophobic core structure in a protein, in general, yields large entropy gains because of the huge increase in the freedom of water molecules, which are assumed to be excluded from the core regions of the protein and shifted to the bulk water region. This is one of the mechanisms by which protein core structures are stabilized).

This substantial energy gain accomplished through the Na^+-Phe interaction in the closed conformation may also contribute to the thermostability of the protein. In contrast, in the open conformation, the broad-ranging hydrophobic interactions between the ligand and Phe16 compensate for the significantly stable core structure in the closed conformation for maintaining the thermostability; thus, under alkaline physiological conditions, which provide an abundance of Na^+ ions, such as in palm oil mill effluent (POME), the structural transition may actually occur.[56] The high conservation of Phe16 in the lipases belonging to the abH15.1 family[57] suggests that the functional roles of the Na^+-Phe interaction proposed in the present study may be commonly employed in this protein family (Figure 7). The alkaline physiological conditions may ensure the formation of the Na^+-Phe complex in the lipase.

In *Pseudomonas* lipase, which is a member of a distinct lipase family, i.e., abH15.2, the phenylalanine residue in the catalytic site in *Geobacillus zalihae* lipase is replaced with leucine (Leu) (this Leu is residue number 17 in *Pseudomonas* lipase), as shown in Figure 7. The crystal structures of *Pseudomonas* lipase revealed that the conformational changes between the closed/open conformations also occur, and the positions of the α5- and α6-helices significantly move.[58,59] The 3-D structure of the open conformation showed that Leu17 also participates in the recognition of the ligand through van der Waals contacts and hydrophobic interactions, leading to the stabilization of the open conformation. However, the large enthalpy gain of the Na^+-π interaction is absent in the closed conformation of the *Pseudomonas* lipase; instead, Leu17 forms hydrophobic interactions with Phe142, Phe146, and Leu149 located on α5, which are all absent in the open conformation, thereby leading to an energy gain in the closed conformation. These interactions in the closed conformation are presumed to overcome those between Leu17 and the ligand in the open conformation, thus substituting for the functional roles of the Na^+-Phe interaction to enable the structural transition in T1 lipase. However, in T1 lipase, the only amino acid residue that interacts with Phe16 on the mobile helix is Phe180, even though the orientations of the side chains of Phe16 in T1 lipase and Leu17 in the *Pseudomonas* lipase are identical. Without the Na^+-π interaction, the hydrophobic aromatic ring of the Phe16 side chain would directly interact with hydrophilic amino acid residues, such as Ser113/His358/Asp317, for preserving the catalytic core structure of T1 lipase. This further confirms our proposed functional roles of the Na^+-π interaction in T1 lipase.

So far, despite many efforts to account for the polarization effects, force fields with broader applications have not yet emerged.[60,61] Recently, the development of a force field for the accurate description of a cation-π interaction was attempted, but it was not effective.[61] A possible reason of the failure might be the introduction of damping functions to determine the parameters of atomic polarizabilities based on ab initio calculations, although several studies have been reported in terms of the improvement of the functions.[62−65] As discussed in this report, we also attempted to optimize the parameters relevant to the polarizable effects to reproduce the potential curve of the Na^+-Phe interaction; however, it was impossible to find values that agreed well with the potential curve obtained using the CCSD(T) calculations. Thus, to the best of our knowledge, the present scheme is currently the only way to perform long-time MD simulations of biological macromolecules including cation-π interactions. In addition, it is generally applicable for the accurate estimation of other interactions involving π systems that standard MM calculations cannot correctly describe.

4. Conclusions

In the present work, using our grid-based representation to evaluate the electrostatic interaction, we proposed the functional roles of the Na^+-Phe interaction in T1 lipase; the significant stabilization energy of the Na^+-Phe interaction is essential for the formation of the stable core structure of the catalytic site, thereby leading to a novel structural element via "Na^+-bridges" for the packing of the hydrophobic aromatic ring (Phe16) and the hydrophilic amino acid residues (Ser113 and His358). While the direct interactions of such residues are energetically unfavorable, the Na^+-bridging interactions are exploited for the stable packing of those residues in the buried protein structure. This may also be crucial for the structural changes from the open to closed conformations, to overcome the large energy gain achieved through the broad-ranging van der Waals contacts and the hydrophobic interactions between the enzyme and the ligand in the open conformation. Thus, the substantial stabilization of the core structure of the catalytic site is established, thereby leading to large gains in both enthalpy and entropy in the closed conformation of T1 lipase. To the best of our knowledge, this is the first study where the detailed functional mechanisms relevant to the Na^+-π interaction have been elucidated at atomic resolution.

Moreover, our grid-based evaluation scheme for cation-π interactions is currently the only way to perform long-time MD simulations with reasonable computational costs. The structural stability of the catalytic site observed in the MD simulation and the convergence of the free energy calculation indicate that the

(56) Ahmad, A. L.; Sumathi, S.; Hammed, B. H. *Adsorp. Sci. Technol.* **2004**, *22*, 75–88.
(57) Fischer, M.; Pleiss, J. *Nucleic Acids. Res.* **2003**, *31*, 319–21.
(58) Lang, D. A.; Mannesse, M. L.; de Haas, G. H.; Verheij, H. M.; Dijkstra, B. W. *Eur. J. Biochem.* **1998**, *254*, 333–340.
(59) Noble, M. E.; Cleasby, A.; Johnson, L. N.; Egmond, M. R.; Frenken, L. G. *FEBS Lett.* **1993**, *331*, 123–128.
(60) Warshel, A.; Kato, M.; Pisliakov, A. V. *J. Chem. Theory Comput.* **2007**, *3*, 2034–2045.
(61) Jorgensen, W. L. *J. Chem. Theory Comput.* **2007**, *3*, 1877–1877.
(62) Thole, B. T. *Chem. Phys.* **1981**, *59*, 341–350.
(63) Holt, A.; Karlstroem, G. *J. Comput. Chem.* **2008**, *29*, 1084–1091.
(64) Jensen, L.; Astrand, P. O.; Osted, A.; Kongsted, J.; Mikkelsen, K. V. *J. Chem. Phys.* **2002**, *116*, 4001–4010.
(65) Burnham, C. J.; Li, J. C.; Xantheas, S. S.; Leslie, M. *J. Chem. Phys.* **1999**, *110*, 4566–4581.

application of our scheme for a description of the Na^+-π interaction does not impair the balanced representation of the force field. This will enable us to understand the detailed mechanisms of the functional roles of cation-π interactions, such as Na^+/K^+-Tyr/Trp/Phe and Cs^+-Trp/Phe interactions, which are widely employed in diverse biological systems, as well as in the lipases from various organisms possessing the conserved Gly-Phe-X-Gly motif.

Acknowledgment. We thank Dr. Hiori Kino for valuable scientific discussions. This work was supported by Grants-in-Aid from the Ministry of Education, Culture, Sports, Science, and Technology (MEXT) under Contract Nos. 19019003 and 21340108. Computations were performed using computer facilities under the "Interdisciplinary Computational Science Program" at the Center for Computational Sciences, University of Tsukuba, the Computer Center for Agriculture, Forestry, and Fisheries Research, MAFF, Japan, and the Supercomputer Center, Institute for Solid State Physics, University of Tokyo.

Supporting Information Available: The table of Cartesian coordinates for the benzene in the Na^+−benzene complexes, the complete citation for ref 29, discussions of the mechanisms of structural disruption observed in the MD simulations with the polarizable and nonpolarizable force fields, and an attempt to find appropriate atomic polarizability to reproduce accurate potential energy curve. This information is available free of charge via the Internet at http://pubs.acs.org.

JA903451B